Submillimolar Detection of Adenosine Monophosphate Using Graphene-Based Electrochemical Aptasensor

Debopam Datta, Xenia Meshik, Souvik Mukherjee, Ketaki Sarkar, Min S. Choi, Mojgan Mazouchi, Sidra Farid, Yung Yu Wang, Peter John Burke, *Member, IEEE*, Mitra Dutta, *Fellow, IEEE*, and Michael A. Stroscio, *Fellow, IEEE*

***Abstract*—In this paper, we present a successful demonstration of a graphene-based field-effect-transistor-like electrochemical nanobiosensor to accurately detect ultralow concentrations of adenosine monophosphate (AMP). Graphene being a two-dimensional material is a suitable option as a sensing element due to its biocompatibility and large surface area. It has also demonstrated surface binding chemistries as well as its ability to serve as a conducting channel. A short 20-base deoxyribonucleic acid (DNA) aptamer is used as the sensing element to ensure that the interaction between the analyte and the aptamer occurs within the Debye length of the electrolyte. The sensor is found to be nonlinear in nature and sensitive in the picomolar (pM) and nanomolar (nM) concentrations of AMP. The linear region of operation is found to be 1 nM–100 μM and percentage change in drain current in this concentration region is calculated as 1.56%/$decade$. A minimum concentration of 10 pM of AMP has been detected using this type of sensor.**

***Index Terms*—Adenosine monophosphate (AMP), DNA aptamer, electrochemical-DNA sensor, graphene ion sensitive FET, Nanosensors.**

I. Introduction

ADENOSINE monophosphate (AMP) is one of the most important compounds in the human body and is created as a metabolic byproduct. AMP, or to be precise cyclic AMP, is responsible for activating the protein kinase A which has a key role in hormonal function and gene transcription. Adenylate kinase and downstream AMP signaling are an integrated metabolic monitoring system which reads the cellular energy state in order to tune and report signals to metabolic sensors [1]. functions including body energy sensing, sleep, hibernation and Metabolic analyses indicate that cellular, interstitial and blood AMP levels are potential metabolic signals associated with vital food intake. Either low or excess AMP signaling has been linked to human diseases such as diabetes, obesity and hypertrophic cardiomyopathy [1]. AMP-activated protein kinase (AMP-K) regulates mitochondrial biogenesis and disposal, autophagy, i.e., self-destruction of cell, cell polarity, cell growth and proliferation. Bacteria and viruses downregulate AMP-K to make the cell vulnerable towards uncontrollable growth which might turn malignant [2]. The ocular AMP level in Diabetic Retinopathy patients shows a variation of 600 nM [3] and blood cyclic AMP level changes by ~ 4 nM in fasting condition [4]. Hence, detection of AMP is a very important task.

There are various detection methods for AMP already reported such as the chronocoulometric method [5], fluorescent and magnetic nano-silica sandwich which uses the principle of fluorescence spectroscopy [6], a biochemical method utilizing conversion of AMP to ATP [7] and micro gravimetric [8]. In this article, we report the detection of AMP using deoxyribonucleic acid (DNA) aptamer and graphene FET based sensing. The sensor used is a liquid gate field effect transistor (FET)-like structure which uses graphene as the channel material and aptamers as a channel property controller. Due to an unprecedented growth in the areas of device fabrication and processing, researchers have been able to successfully fabricate and test devices in the nanoscale regime with high precision and reliability which are comparable in size with biological structures and have paved the way in their integration. Researchers have tried to use FETs as the basis for real time bio-sensing and label-free detection, low detection limits and simple integration using microelectronic fabrication techniques [9]. Potential applications, developments and impact of integrated biological-semiconductor devices has been discussed by Stroscio *et al.* [10]. In our experiments we have used liquid gated FET which contains a silver/silver chloride microelectrode gate unlike traditional metal oxide semiconductor gate FET transistor.

Aptamers are single-stranded DNA or ribonucleic acid (RNA) (ssDNA or ssRNA) molecules, which can bind to pre-selected targets including proteins, peptides, and ions with high affinity

Manuscript received November 1, 2016; revised December 16, 2016; accepted December 30, 2016. Date of publication January 4, 2017; date of current version March 8, 2017. This work was supported by the Army Research Office under MURI Grant W911NF-11-1-0024. The review of this paper was arranged by Associate Editor A. Ural.

D. Datta, S. Mukherjee, K. Sarkar, M. S. Choi, M. Mazouchi, and S. Farid are with the Department of Electrical and Computer Engineering, University of Illinois at Chicago, Chicago, IL 60607 USA (e-mail: ddatta2@uic.edu; smukhe8@uic.edu; ksarka3@uic.edu; mchoi29@uic.edu; mmazou2@uic.edu; sidrafarid@gmail.com).

X. Meshik is with the Department of Bioengineering, University of Illinois at Chicago, Chicago, IL 60607 USA (e-mail: xmeshik@gmail.com).

Y. Y. Wang and P. J. Burke are with the Department of Chemical Engineering and Materials Science, University of California—Irvine, Irvine, CA 92697 USA (e-mail: willwang107@gmail.com; pburke@uci.edu).

M. Dutta is with the Department of Electrical and Computer Engineering, and also with the Department of Physics, University of Illinois at Chicago, Chicago, IL 60607 USA (e-mail: dutta@uic.edu).

M. A. Stroscio is with the Department of Electrical and Computer Engineering, the Department of Bioengineering, and the Department of Physics, University of Illinois at Chicago, Chicago, IL 60607 USA (e-mail: stroscio@uic.edu).

Color versions of one or more of the figures in this paper are available online at http://ieeexplore.ieee.org.

Digital Object Identifier 10.1109/TNANO.2016.2647715

and specificity. The adenosine-5'-monophosphate (AMP) DNA aptamer was first reported by Huizenga *et al.* in 1995 [17]. This aptamer was investigated for functional adenosine binding sequences in which the guanosine-rich region forms G-quartet to capture AMP molecules. The AMP binds to the DNA aptamer via H-bonds formed between adenosine residues of AMP [17], [18] and the nucleotides of DNA. In the presence of the aforementioned groups, the highest binding affinity can be observed. Recently, aptamers as a new class of recognition components have attracted tremendous attention and emerged as a promising alternative to conventional recognition elements analogous to antibodies [19]. Since the concept of aptamer was introduced [20], [21], numerous aptamers have been reported, which could specifically bind to various target ligands such as small organic molecules, metal ions, proteins and cells [19].

In recent years, there has been an increasing trend of aptamer-based bio-sensing using 1D and 2D nanomaterials as channel components. Though 1D materials are frequently described as having advantages like higher sensitivity and biocompatibility than 2D materials but they generally require more sophisticated fabrication techniques. For example, fabricating a nanowire FET requires isolation and alignment of a single nanowire, creating metal pads (contacts) with almost zero contact resistance is a very cumbersome task [22]. On the other hand, graphene being a 2D material is of particular interest in bio-sensing due to its 2D structure, biocompatibility, effective ligand surface binding chemistries and graphene can be easily transferred by simple scotch-tape method from graphite or PDMS stamping from copper foil. As a result, it has been considered in this aptamer-based work. Aptamers are single-stranded DNA or RNA molecules which bind to specific target analytes like metal ions [11], [12], proteins [13], and organic and inorganic molecules [14]. Aptamers have advantages over antibody-based immunoassays [15]. In this article, we report a label free FET-like electrochemical biosensor having graphene channel for the detection of AMP.

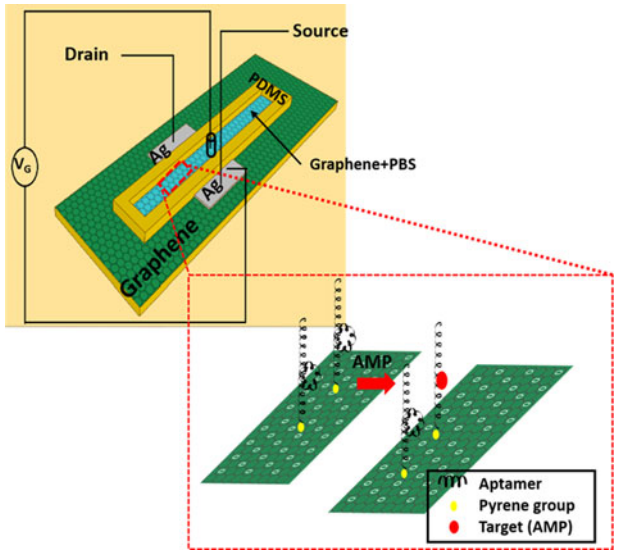

Fig. 1. This schematic diagram of the device (left) and enlarged picture of the graphene interface with the aptamer which detects AMP via conformational change of the aptamer (black coiled structure) attached on the surface of the graphene sheet (green area). Most of the graphene is only present beneath the well region.

II. Experimental Details

A. Device Description

Liquid gated graphene field effect transistor is used as the electrochemical biosensor device in our experiments. The growth and fabrication of the devices were performed by Burke *et al.* and have been presented in a previous article [16]. High purity monolayer graphene was grown on Cu foil using low pressure chemical vapor deposition (LPCVD). The graphene was then transferred using poly(-dimethyl siloxane) (PDMS) which was used as the substrate for the FET. This technique ensured transfer of a contamination free graphene film. Raman Spectroscopy was done on the graphene film. The ratio of the peak intensity of the G band to 2D band was $\sim$0.3 which suggested the existence of a monolayer graphene. The topographical analysis was performed using SEM and AFM on the graphene structure to detect any cracks or folds. Fig. 1 shows the device layout of the liquid gate field effect transistor(FET). A rectangular PDMS well structure was placed on the previously transferred graphene film on the PDMS substrate. The well acts as a fillister containing ionic solutions with conducting graphene layer at the base, and the average well size is ca. 0.8 cm $\times$ 0.4 cm $\times$ 0.2 cm. Source and drain electrodes were formed on either side of the PDMS fillister using silver solution. An Ag/AgCl reference electrode (Microelectrode Inc., Bedford, NH) was placed in the ionic solution in the well which acted as the gating electrode. Binding of the aptamer to the graphene in the ionic solution was done to detect the target ions. Due to the reaction between the target ions and the aptamer, the latter undergoes a conformational change which is reflected in the transfer characteristics of the liquid gated FET-like transistor.

B. Preparing Aptamer Modified Graphene Surface

75 μM of aptamer solution is diluted to 15 μM of dimethylformamide (DMF) (Sigma Aldrich, St. Louis, MO). 50 μL of that solution was placed in the FET fillister and kept at room temperature for 3 hours. In order to remove excess and unbounded aptamers, the well was washed with PBS four to five times. FETs for control experiments were also prepared following the same procedure but no aptamer solution is added in order to validate that AMP-aptamer complex is the primary cause behind device transfer curve alteration if any. The wells were kept filled with 50 μL PBS all the times and experiments were conducted on the same day to avoid adhesion of the aptamer to the graphene surface.

C. Sensing Procedure by Monitoring Drain Current

In these experiments, the sensing of different concentration of the analyte is accomplished by tracking the change in Dirac point drain current versus Dirac point gate voltage. To perform the experiment, the gate to source voltage was varied from -1 V to 1 V, keeping the drain to source voltage fixed at 0.3 V.

TABLE I
SEQUENCE OF AMP DNA APTAMERS USED IN PREVIOUSLY PUBLISHED STUDIES

Number	Aptamer sequence (5'—> 3')	Reference
1	GGCTT**GGGGGAGTATTGCGGAGGAA**AGCGGCCCTGCTGAAG	17
2	ACCT**GGGGAGTAAAGCGGAGGA**AGGT	23
3	CCT**GGGGGAGTATTGCGGAGGAA**GG	24
4	GGGUUGGGAAGAAACUGUGGCACUUCGGUGCCAGCAACCC (RNA based)	25, 26

The gate voltage was applied via Ag/AgCl reference microelectrode, and the drain-source current was measured using the Agilent 4156B semiconductor parameter analyzer. AMP obtained from Sigma Aldrich, St. Louis, MO was dissolved in PBS and different concentrations were added to the well to observe the change in the drain current. The same experiment is repeated on 4 samples in order to obtain statistically significant result. We performed separate control experiments by adding AMP in the FET fillister without any aptamer present. We also performed additional control experiments by adding L-cysteine, Guanosine mono-phosphate (GMP), Uridine mono-phosphate (UMP) to the aptamer functionalized well. Control Experiments are also implemented onto 3 different samples. Any non-target molecule should serve as a control substance but L-cysteine is of special significance since it is comparable in size with AMP whereas GMP and UMP are structurally similar to AMP.

III. RESULTS AND DISCUSSION

A. Selection of Aptamer and Secondary Folding of the Aptamer

The aptamer used in our experiment contains the common 20 DNA base pair sequence similar to the aptamer used by Huizenga *et al.* and Lin *et al.* [17] shown in the Table I. The most important consideration is to keep the length of the aptamer less than the Debye length of the buffer solution, which is phosphate buffer saline (PBS). As seen in Table I, there is a consistent nucleotide motif in three of the four aptamers used in previously-published studies, and therefore we assume that this motif is the sequence involved in binding AMP. Hence aptamer with 5'-GGGGGAGTATTGCGGAGGAA-3' (obtained from Biosearch Technologies) sequence with pyrene modification on 5' end is used in order to satisfy Debye length criterion. The secondary structure of the selected aptamer is shown in Fig. 4(b) based on minimum Gibbs free energy criterion using Mfold software. The aptamer-graphene binding is facilitated by the pyrene group attached to the 5' end of the aptamer via π-π stacking.

B. Immobilization of Aptamers on the Graphene Surface

The aptamers should be immobilized on the graphene surface such that they remain within the Debye length of the electrolyte. There are various methods to verify the immobilization of the aptamers such as quantum dot tagging of the aptamers [11] or SEM imaging [29]. However, AFM topographical imaging is an easy and reliable method to ensure the proper binding of the aptamers on the graphene surface. Fig. 2(a) shows a 3D height profile of the graphene surface with aptamers bound to it, unlike Fig. 2(b) which shows height profile of the graphene surface devoid of aptamers. The aptamers we have used are 20 base pairs long. Some of the spikes in 3D image show a higher value which probably depicts the agglomeration of aptamers in a specific region during AFM imaging only. The uneven surface in Fig. 2 might be attributed to the inherent surface roughness of the PDMS and residue resulted from binding process of the aptamer.

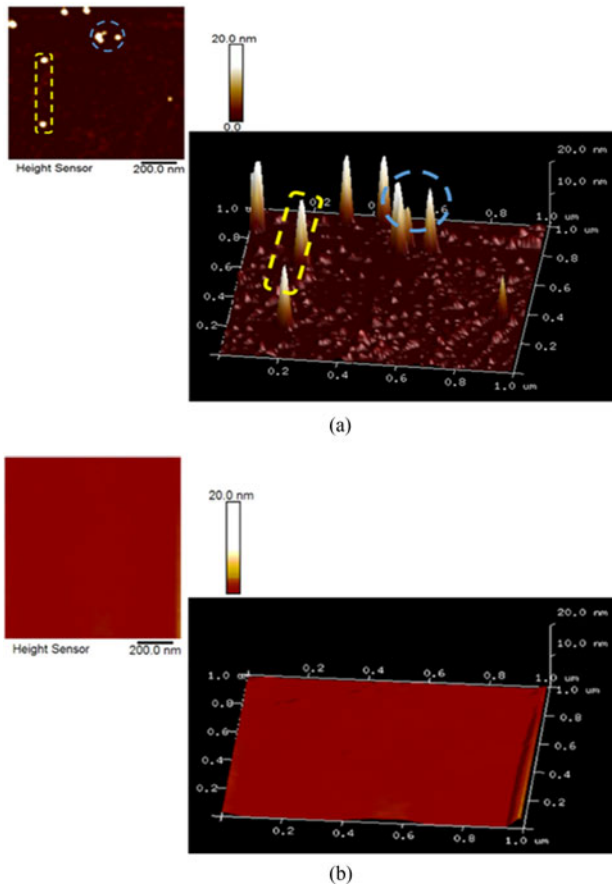

Fig. 2. a) The 3D AFM image of a graphene sheet with aptamers bound to it. The spikes in the sheet refers to the aggregation of aptamers on the graphene sheet. The AFM is done on the sample after binding the aptamers. b) The 3D image of graphene devoid of aptamers are shown which is captured before modifying the graphene surface. For both of the figures the 2D projection or top view is given in the inset and the scan area shown is 1 μm $\times$ 1 μm. The aggregation of the aptamers might be due to the fact that during AFM the fillister does not contain any PBS to disperse the aptamers.

C. Liquid Gated Graphene FET Device Characteristics

Conductivity and functionality of the FET-like devices have been tested by adding PBS in the well and measuring the drain current (Id), gate voltage (Vg) and drain voltage (Vd).

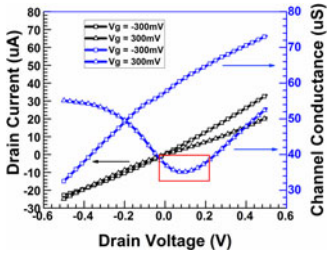

Fig. 3. Plot of Id vs Vd for gate voltage 300 mV (in black triangle) and −300 mV (in black square). Also shown is the channel conductance for the two different values of gate voltage (blue). The red region shows the inversion of channel conductance nature for Vg = 300 mV. For negative gate voltage the channel nature does not inverts within these value of drain voltage.

The device transfer characteristics i.e. gate voltage (Vg) vs. drain current (Id) is measured using an HP4156B parameter analyzer. The linear nature of Vd and Id is expected for a continuous graphene sheet and used as a criterion for usability of that particular sensor. The slope obtained from the Id-Vd curve represents the average channel resistance for the particular sensor. The slope of the Id-Vd curve at $\mathrm{Vg} = 300\,\mathrm{mV}$ comes out to be 43.28 μS, hence the channel resistance can be calculated ca. 23 kΩ. The contact resistance between graphene and silver electrode in the source and drain region is given as 917 Ω [16] which is much smaller than the channel resistance; hence, we can ignore the voltage drop across the contact resistance. The variation of drain current occurs due to modification of channel nature, i.e., n-type and p-type for a different combination of gate-source voltage (Vg) and Vd. The variation of channel conductance shown in Fig. 3 is observed because the change in drain voltage polarity inverts the carrier type in the channel. The variation of conductance in two regions occurs as a result of the difference in electron and hole mobility. It is observed that when positive drain to source voltage is increased the channel inversion takes place at a higher gate voltage value (data not shown). The phenomenon is observed because in order to invert the channel, a higher gate voltage is required for elevated drain to source voltage.

D. Graphene-Based Detection of AMP

After binding the aptamer, the drain voltage was kept fixed at 0.3 V and the transfer characteristics was measured for the sensor. The curve for the same exhibits a minimum Id point known as Dirac point (DP). The drain current response with variation in gate voltage is shown in Fig. 5. In the region to the right of the DP, the FET channel behaves as n-type, i.e., electrons are the majority carriers and in the left region of DP it behaves as p-type. The transconductance curve in Fig. 4(a) explains the above mentioned fact. For accurate sensing with ionic liquid gated FET the two most important factors are Debye length of the electrolyte and the quality of the graphene sheet. 0.01x PBS solution used as the gate electrolyte in the experiments have a Debye length of $\sim 8.25\,\mathrm{nm}$; hence, it is adequate for sensing using short 6-8 nm long aptamers [30]. When AMP binds to the aptamer it undergoes a conformational change [17] which in turn modulates the charge (expressed as drain current) in the graphene. As AMP

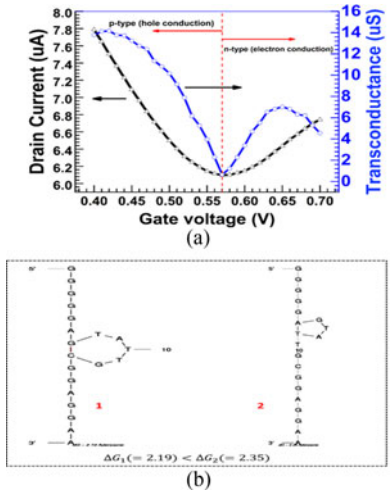

Fig. 4. a) The transconductance and drain current vs. gate voltage plot for drain voltage = 300 mV illustrates the channel characteristics. The right side region of the DP (red dashed line) shows the n-type conduction and left half is p-type. b) Most probable two conformations of the aptamer used; modelled using M-fold software (considering sodium concentration to be = 0.00138 M (0.01 × PBS)).

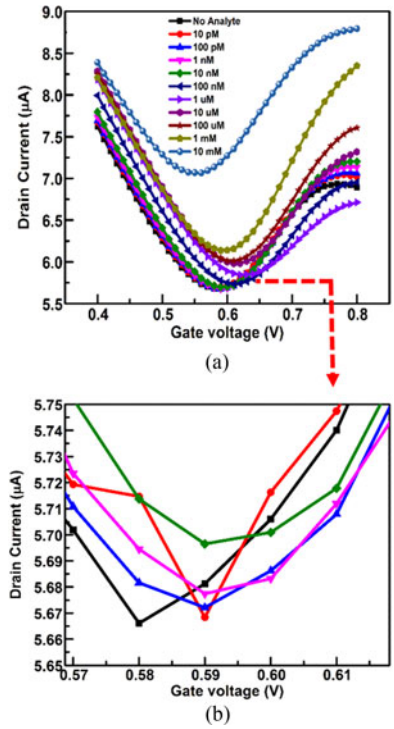

Fig. 5. a) The change in the Id-Vg transfer curve for progressive addition of AMP from 10 pM to 10 mM. The Dirac point current value increases with higher AMP concentration. b) The zoomed in graphs for 10 pM to 10 nM in the Dirac point region for the sensor.

is added progressively from 10 pM to 10 mM to the FET well, the drain current value at DP increases as shown in Fig. 6(a). The p-type current and Dirac point current both show a constant increase with AMP addition due to the fact that more aptamers are conformed within Debye length of PBS and DNA aptamers contain a heavily negatively charged phosphate backbone. This DNA conformation enhances the unscreened charge quantity in

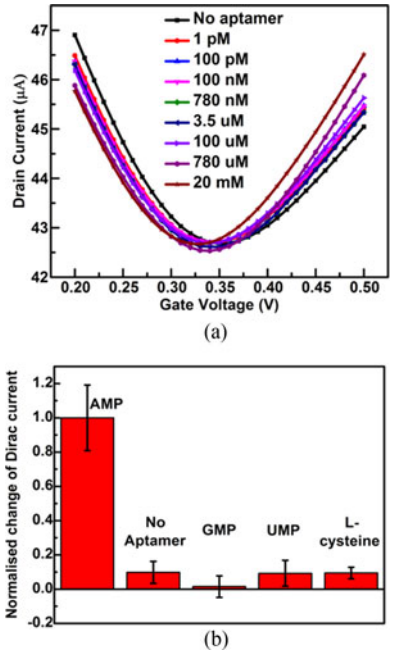

Fig. 6. a) The variation of drain current when AMP is added without the presence of DNA aptamer and b) selectivity of the sensor towards AMP in presence of aptamer, compared to GMP, UMP, L-cysteine and AMP without aptamer attached to the graphene sheet for the range of 10 pM to 10 mM.

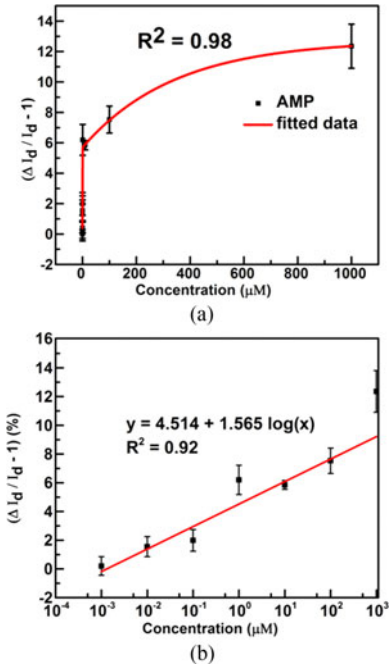

Fig. 7. a) The drain current at Dirac point vs. concentration curve with error bar for calculating the sensitivity of the sensor. The fitted data exhibits a nonlinear relationship between drain current and concentration, where concentration is varied from 0 M to 1 mM. b) The variation of drain current in dynamic range (1 nM to 100 μM) of the sensor is linear (R2 = 0.92) with concentration which determines the sensitivity of the sensor.

Debye length which increases the free carrier concentration in graphene and we observe an increase in current.

E. Selectivity of the Graphene Sensor

In order to provide an indication of the sensor's selectivity towards AMP, we conducted four control experiments as explained before in Section II-C keeping all the conditions identical to the target experiment. The amount of L-cysteine, GMP and UMP added are similar as target and environment of the of experiments are kept identical in order to maintain uniformity. The amount of L-cysteine, GMP and UMP are varied from 10 pM to 10 mM similar to the AMP to obtain a comparison between target and control. According to Fig. 6(b) the change in DP current is maximum for the case of AMP compared to control experiment result. The control experiments lead to the conclusion that our sensor is suitable for detecting AMP in presence of L-cysteine. The significant change in current for AMP in the presence of aptamer shows that the sensor is also selective to AMP but only if aptamers are present.

F. Sensitivity and Limit of Detection of the Sensor

The sensitivity of our sensor platform is calculated by obtaining first order derivative of the calibration curve (Fig. 7(a)). A nonlinear trend is observed in the calibration curve where the percentage change of drain current at DP I_{Dirac} vs Gate voltage is shown for 0 M to 1 mM AMP concentration. The response curve has been fitted with a third order exponential decay model with a strong correlation ($\mathrm{R}^2 = 0.98$) and it appears to be of the form:

$$\begin{aligned}\text{Percentage change in } I_{Dirac} = {} & 12.737 - 5.27 \exp\left(\frac{-x}{0.242}\right) \\ & - 2.564 \exp\left(\frac{-x}{342.03}\right) \\ & - 4.477 \exp\left(\frac{-x}{342.65}\right) \qquad (1)\end{aligned}$$

where x is expressed in μM. The sensor is found to be highly non-linear in nature, which can be observed graphically from calibration curve plot and inferred quantitatively from calibration equation. Due to highly non-linear behavior, the sensitivity of the sensor is observed to be monotonically decreasing with concentration. Though the sensor exhibits non-linear behavior, for a range of 1 nM to 100 μM the sensor shows a linear behavior with logarithm of AMP concentration. For the linear region, the percentage change of I_{Dirac} is found to be $1.56\,\%/decade$ change of AMP concentration which can be inferred as sensitivity of the sensor. Experiments performed on multiple devices reveal that the change in drain current value at DP for 10 pM concentration of AMP is significantly higher compared to the noise floor of respective blank samples. Hence 10 pM is concluded as the reliably detected minimum concentration of AMP for this sensor. In case of a diabetic patient the ocular AMP level and serum AMP level changes by 600 nM and 4 nM respectively as mentioned in Section I, which lie within the dynamic range of our reported sensor. Hence the sensor can be employed in medical anomaly detection scenarios like diabetes.

IV. Conclusion

In this work, we have successfully demonstrated a unique liquid gated FET-like nanosensor and its effectiveness in detecting ultralow concentrations of AMP. The relevance of the sensor in medical detection field has also been mentioned. The sensor uses the increase in electron transfer efficiency property of monolayer graphene, which is mediated by folding of the aptamer upon addition of AMP. Several advantages of the sensor include: label free detection, simplistic design, higher stability, good selectivity and sensitivity and very low detection limit. The efficiency of the sensor platform quantified by the sensitivity, is higher in the pico-molar and nano-molar region, and gradually decreases for micro and millimolar concentrations of AMP. Among previously reported methods for detecting AMP, Tanaka *et al.* [7] has achieved a minimum detection of 100 nM concentration comparable to our sensor and operating range of 0.1 μM to 0.1 mM. Sallacan *et al.* [8] has reported AMP sensor with a LOD of 0.1 μM and dynamic range of 0.1 μM to 1 mM. Similar range of detection limit has also been reported by Shen *et al.* [5] and Shon et. al [6]. Additionally, our sensor requires a small sample volume restricted by the volume of the fillister which varies from 60 to 80 μL to display the result; hence, it is optimum for different medical testing procedures. Another advantage is that one can easily detect another analyte on the same graphene platform just by changing the aptamer sequence.

Acknowledgment

The authors would also like to thank the Nanotechnology Core Facility (NCF) at University of Illinois at Chicago for providing clean room facilities to perform AFM and current-voltage measurements.

References

[1] P. Dzeja and A. Terzic, "Adenylate kinase and AMP signaling networks: Metabolic monitoring, signal communication and body energy sensing," *Int. J. Mol. Sci.*, vol. 10, pp. 1729–1772, 2009.

[2] D. G. Hardie, "AMP-activated protein kinase—An energy sensor that regulates all aspects of cell function," *Genes Develop.*, vol. 25, no. 18, pp. 1895–1908, 2011.

[3] S. Loukovaara, S. Sahanne, S. Jalkanen, and G. Yegutkin, "Increased intravitreal adenosine 5′-triphosphate, adenosine 5′-diphosphate and adenosine 5′-monophosphate levels in patients with proliferative diabetic retinopathy," *Acta Ophthalmologica*, vol. 93, no. 1, pp. 67–73, 2015.

[4] J. Drexler, A. Liu, and A. Foti, "Fasting plasma cyclic AMP levels in an adult diabetic and non-diabetic group," *Acta Diabetologica*, vol. 14, no. 3–4, pp. 112–118, 1977.

[5] L. Shen *et al.*, "A chronocoulometric aptamer sensor for adenosine monophosphate," *Chem. Commun.*, vol. 22, no. 21, pp. 2169–2171, 2007.

[6] Y. Song, C. Zhao, J. Ren, and X. Qu, "Rapid and ultra-sensitive detection of AMP using a fluorescent and magnetic nano-silica sandwich complex," *Chem. Commun.*, vol. 15, pp. 1975–1977, 2009.

[7] S. Tanaka, A. Kuroda, J. Kato, T. Ikeda, N. Takiguchi, and H. Ohtake, "A sensitive method for detecting AMP by utilizing polyphosphate-dependent ATP regeneration and bioluminescence reactions," *Biochem. Eng. J.*, vol. 9, no. 3, pp. 193–197, 2001.

[8] N. Sallacan, M. Zayats, T. Bourenko, A. B. Kharitonov, and I. Willner, "Imprinting of nucleotide and monosaccharide recognition sites in acrylamidephenylboronic acid-acrylamide copolymer membranes associated with electronic transducers," *Anal. Chem.*, vol. 74, no. 3, pp. 702–712, 2002.

[9] J. Kim *et al.*, "Fabrication of high-performance ultrathin In_2O_3 film field-effect transistors and biosensors using chemical lift-off lithography," *ACS Nano*, vol. 9, no. 4, 4572–4582, 2015.

[10] M. A. Stroscio and M. Dutta, "Integrated biological-semiconductor devices," *Proc. IEEE*, vol. 93, no. 10, pp. 1772–1783, Oct. 2005.

[11] K. Xu, X. Meshik, B. M. Nichols, E. Zakar, M. Dutta, and M. A. Stroscio, "Graphene-and aptamer-based electrochemical biosensor," *Nanotechnology*, vol. 25, no. 20, Apr. 2014, Art. no. 205501.

[12] Z. Jiang, Y. Zhang, A. Liang, C. Chen, J. Tian, and T. Li, "Free-labeled nanogold catalytic detection of trace UO2+ based on the aptamer reaction and gold particle resonance scattering effect," *Plasmonics*, vol. 7, pp. 185–190, 2012.

[13] N. Hamaguchi, A. Ellington, and M. Stanton, "Aptamer beacons for the direct detection of proteins," *Anal. Biochem.*, vol. 294, pp. 126–131, 2011.

[14] H. Zhang, B. Jiang, Y. Xiang, Y. Zhang, Y. Chai, and R. Yuan, "Aptamer/quantum dot-based simultaneous electrochemical detection of multiple small molecules," *Anal. Chim. Acta*, vol. 688, pp. 99–103, 2011.

[15] K. Maehashi, T. Katsura, K. Kerman, Y. Takamura, K. Matsumoto, and E. Tamiya, "Label-free protein biosensor based on aptamer-modified carbon nanotube field-effect transistors," *Anal. Chem.*, vol. 79, no. 2, pp. 782–787, 2007.

[16] Y. Y. Wang and P. J. Burke, "A large-area and contamination-free graphene transistor for liquid-gated sensing applications," *Appl. Phys. Lett.*, vol. 103, no. 5, 2013, Art. no. 052103.

[17] D. E. Huizenga and J. W. Szostak, "A DNA aptamer that binds adenosine and ATP," *Biochemistry*, vol. 34, no. 2, pp. 656–665, Jan. 1995.

[18] S. Nonin-Lecomte, C. H. Lin, and D. J. Patel, "Additional hydrogen bonds and base-pair kinetics in the symmetrical AMP-DNA aptamer complex," *Biophys. J.*, vol. 81, no. 6, pp. 3422–3431, 2001.

[19] K. Han, Z. Liang, and N. Zhou, "Design strategies for aptamer-based biosensors," *Sensors*, vol. 10, pp. 4541–4557, 2010.

[20] A. D. Ellington and J. W. Szostak, "In vitro selection of RNA molecules that bind specific ligands," *Nature*, vol. 346, no. 6287, pp. 818–822, 1990.

[21] L. C. Bock, L. C. Griffin, J. A. Latham, E. H. Vermaas, and J. J. Toole, "Selection of single-stranded DNA molecules that bind and inhibit human thrombin," *Nature*, vol. 355, pp. 564–566, 1992.

[22] K. S. Kim, H. S. Lee, J. A. Yang, M. H. Jo, and S. K. Hahn, "The fabrication, characterization and application of aptamer-functionalized Si-nanowire FET biosensors," *Nanotechnology*, vol. 20, no. 23, 2009, Art. no. 235501.

[23] C. H. Lin and D. J. Patel, "Structural basis of DNA folding and recognition in an AMP-DNA aptamer complex: Distinct architectures but common recognition motifs for DNA and RNA aptamers complexed to AMP," *Chem. Biol.*, vol. 4, no. 11, pp. 817–832, 1997.

[24] P. Baaske, C. J. Wienken, P. Reineck, S. Duhr, and D. Braun, "Optical thermophoresis for quantifying the buffer dependence of aptamer binding," *Angewandte Chemie Int. Ed. Engl.*, vol. 49, no. 12, pp. 2238–2241, 2010.

[25] T. Nguyen, R. Pei, M. Stojanovic, and Q. Lin, "Demonstration and characterization of biomolecular enrichment on microfluidic aptamer-functionalized surfaces," *Sens. Actuators B, Chem.*, vol. 155, no. 1, pp. 58–66, 2011.

[26] D. Patel *et al.*, "Structure, recognition and adaptive binding in RNA aptamer complexes," *J. Mol. Biol.*, vol. 272, no. 5, pp. 645–664, 1997.

[27] S. Mukherjee *et al.*, "A graphene and aptamer based liquid gated FET-like electrochemical biosensor to detect adenosine triphosphate," *IEEE Trans. NanoBiosci.*, vol. 14, no. 8, pp. 967–972, Dec. 2015.

[28] S. Farid *et al.*, "Detection of Interferon gamma using graphene and aptamer based FET-like electrochemical biosensor," *Biosens. Bioelectron.*, vol. 71, pp. 294–299, 2015.

[29] Y. Wan, Y. Wang, J. Wu, and D. Zhang, "Graphene oxide sheet-mediated silver enhancement for application to electrochemical biosensors," *Anal. Chem.*, vol. 83, no. 3, pp. 648–653, 2010.

[30] A. Vacic, J. Criscione, N. Rajan, E. Stern, T. Fahmy, and M. Reed, "Determination of molecular configuration by Debye length modulation," *J. Amer. Chem. Soc.*, vol. 133, no. 35, pp. 13886–13889, 2011.

[31] H. Loock and P. Wentzell, "Detection limits of chemical sensors: Applications and misapplications," *Sens. Actuators B, Chem.*, vol. 173, pp. 157–163, 2012.

Debopam Datta received the B.E. degree in electronics and telecommunication engineering from Indian Institute of Engineering, Science and Technology, Shibpur, India (formerly Bengal Engineering and Science University, Shibpur), in 2013. He is currently working toward the doctoral studies in electrical engineering at the University of Illinois at Chicago, Chicago, IL, USA.

Xenia Meshik received the B.A. degree in biology from Washington University, St. Louis, MO, USA, in 2008. She is currently working toward the Ph.D. degree in bioengineering at the University of Illinois at Chicago, Chicago, IL, USA, studying quantum dot- and aptamer-based nanostructures for biological applications.

Souvik Mukherjee received the B.Tech. degree in electronics and communication engineering from West Bengal University of Technology, Kolkata, India, in 2012. He is currently working toward the Ph.D. degree at the University of Illinois at Chicago, Chicago, IL, USA.

Since October 2015, he has been working as a Guest Graduate Appointee in the Nuclear Engineering division of Argonne National Laboratory, in which he is engaged in research on semiconductor oxide nanostructures for their use in electromagnetic sensing applications as well as generation of THz radiation.

Ketaki Sarkar received the B.Sc. degree in physics (Hons.) from the University of Calcutta, Kolkata, India, and the B.Tech. degree in electronics and instrumentation from Jadavpur University, Kolkata, India, in 2007 and 2010, respectively. She is currently working toward the Ph.D. degree at the University of Illinois at Chicago, Chicago, IL, USA, where her work is focused on the optical characterization of nanowire.

Min S. Choi received the B.S. degrees in engineering physics and business administration from the University of Colorado at Boulder, Boulder, CO, USA. He is currently working toward the Ph. D. degree in electrical engineering at the University of Illinois at Chicago, Chicago, IL, USA, under supervision of Dr. Michael A. Stroscio.

Mojgan Mazouchi received the B.S. degree in electrical engineering from K. N. Toosi University of Technology, Tehran, Iran, in 2012. She is currently working toward the Ph.D. degree in the Department of Electrical and Computer Engineering, University of Illinois at Chicago, Chicago, IL, USA. Her current research focuses on nanostructured semiconductor materials and devices.

Sidra Farid is currently working toward the Ph.D. degree in the Department of Electrical and Computer Engineering, University of Illinois at Chicago, Chicago, IL, USA.

Yung Yu Wang is with the Chemical Engineering and Materials Science Department, University of California—Irvine, Irvine, CA, USA.

Peter John Burke (M'02) received the Ph.D. degree in physics from Yale University, New Haven, CT, USA, in 1998.

From 1998 to 2001, he was a Sherman Fairchild Postdoctoral Scholar in physics in the California Institute of Technology, Pasadena, CA, USA. Since 2001, he has been a faculty member in the Department of Electrical Engineering and Computer Science, University of California—Irvine, Irvine, CA, USA.

Mitra Dutta (F'99) received the Ph.D. degree from the University of Cincinnati, Cincinnati, OH, USA, in 1981.

She is currently the Vice Chancellor for Research and a Distinguished Professor at the University of Illinois at Chicago, Chicago, IL, USA. She holds an appointment in electrical and computer engineering, and is an Adjunct Professor of physics at the University of Illinois at Chicago. She has published in engineering and the physical sciences more than 200 journal articles, coauthored a book, 24 patents, and coedited four books.

Dr. Dutta is a Fellow of the American Association for the Advancement of Science, the Optical Society of America, the Society of Women Engineers, and the Emeritus of the Army Research Laboratory. She received the 2000 IEEE-USA Harry Diamond Memorial Award, and the 2003 National Achievement Award of the Society of Women Engineers.

Michael A. Stroscio (F'92) received the Ph.D. degree from Yale University, New Haven, CT, USA, in 1974.

He is currently the Richard and Loan Hill Professor of engineering, a Professor of bioengineering, a Professor of electrical and computer engineering, and an Adjunct Professor of physics at the University of Illinois at Chicago, Chicago, IL, USA. He has published in engineering and the physical sciences more than 300 journal articles, coauthored three books, more than 12 patents, and coedited five books.

Dr. Stroscio is a Fellow of the American Association for the Advancement of Science, the American Physical Society, the Yale Science and Engineering Association, and the Emeritus of the Army Research Laboratory. He received the 1998 IEEE-USA Harry Diamond Memorial Award.